medRxiv preprint doi: https://doi.org/10.1101/2025.01.14.24319457; this version posted January 17, 2025. The copyright holder for this preprint (which was not certified by peer review) is the author/funder, who has granted medRxiv a license to display the preprint in perpetuity.
It is made available under a CC-BY-NC-ND 4.0 International license .

What is the best brain state to predict autistic traits?

Authors

Corey Horien[1,2,3]*, Francesca Mandino[4], Abigail S. Greene[2,5], Xilin Shen[4], Kelly Powell[6], Angelina Vernetti[6], David O'Connor[7], James C. McPartland[6,8], Fred R. Volkmar[6,8], Marvin Chun[8,9], Katarzyna Chawarska[6,10,11], Evelyn M.R. Lake[4,9,12], Monica D. Rosenberg[13,14], Theodore Satterthwaite[1,3,16], Dustin Scheinost[4,6,9,10,15], Emily Finn[17], R. Todd Constable[2,4,12,15,18]*

Affiliations

[1]Department of Psychiatry, University of Pennsylvania, Philadelphia, PA, USA

[2]MD-PhD Program, Yale School of Medicine, New Haven, CT, USA

[3]Penn Lifespan Informatics and Neuroimaging Center (PennLINC), University of Pennsylvania, Philadelphia, PA, USA

[4]Department of Radiology and Biomedical Imaging, Yale School of Medicine, New Haven, CT, USA

[5]Department of Psychiatry, Brigham and Women's Hospital, Boston, MA, USA

[6]Child Study Center, Yale School of Medicine, New Haven, CT, USA

[7]BioMedical Engineering and Imaging Institute, Icahn School of Medicine at Mount Sinai, New York, NY, USA

[8]Department of Psychology, Yale University, New Haven, CT, United States

[9]Wu Tsai Institute, Yale University, New Haven, CT, USA

[10]Department of Statistics and Data Science, Yale University, New Haven, CT, USA

[11]Department of Pediatrics, Yale School of Medicine, New Haven, CT, USA

NOTE: This preprint reports new research that has not been certified by peer review and should not be used to guide clinical practice.

medRxiv preprint doi: https://doi.org/10.1101/2025.01.14.24319457; this version posted January 17, 2025. The copyright holder for this preprint (which was not certified by peer review) is the author/funder, who has granted medRxiv a license to display the preprint in perpetuity.
It is made available under a CC-BY-NC-ND 4.0 International license .

[12]Department of Biomedical Engineering, Yale University, New Haven, CT, USA

[13]Department of Psychology, University of Chicago, Chicago, IL, USA

[14]Neuroscience Institute, University of Chicago, Chicago, IL, USA

[15]Interdepartmental Neuroscience Program, Yale University, New Haven, CT, USA

[16]Penn-CHOP Lifespan Brain Institute, University of Pennsylvania, Philadelphia, PA, USA.

[17]Department of Psychological and Brain Sciences, Dartmouth College, Dartmouth, NH, USA

[18]Department of Neurosurgery, Yale School of Medicine, New Haven, CT, USA

*Corresponding authors:

Corey Horien

Psychiatry Office of Education

3535 Market Street, Suite 200

Philadelphia, PA 19104

corey.horien@pennmedicine.upenn.edu

R. Todd Constable

Magnetic Resonance Research Center

300 Cedar St

PO Box 208043

New Haven, CT 06520-8043

todd.constable@yale.edu

medRxiv preprint doi: https://doi.org/10.1101/2025.01.14.24319457; this version posted January 17, 2025. The copyright holder for this preprint (which was not certified by peer review) is the author/funder, who has granted medRxiv a license to display the preprint in perpetuity.
It is made available under a CC-BY-NC-ND 4.0 International license .

Abstract

Autism is a heterogeneous condition, and functional magnetic resonance imaging-based studies have advanced understanding of neurobiological correlates of autistic features. Nevertheless, little work has focused on the optimal brain states to reveal brain-phenotype relationships. In addition, there is a need to better understand the relevance of attentional abilities in mediating autistic features. Using connectome-based predictive modelling, we interrogate three datasets to determine scanning conditions that can boost prediction of clinically relevant phenotypes and assess generalizability. In dataset one, a sample of youth with autism and neurotypical participants, we find that a sustained attention task (the gradual onset continuous performance task) results in high prediction performance of autistic traits compared to a free-viewing social attention task and a resting-state condition. In dataset two, we observe the predictive network model of autistic traits generated from the sustained attention task generalizes to predict measures of attention in neurotypical adults. In dataset three, we show the same predictive network model of autistic traits from dataset one further generalizes to predict measures of social responsiveness in data from the Autism Brain Imaging Data Exchange. In sum, our data suggest that an in-scanner sustained attention challenge can help delineate robust markers of autistic traits and support the continued investigation of the optimal brain states under which to predict phenotypes in psychiatric conditions.

medRxiv preprint doi: https://doi.org/10.1101/2025.01.14.24319457; this version posted January 17, 2025. The copyright holder for this preprint (which was not certified by peer review) is the author/funder, who has granted medRxiv a license to display the preprint in perpetuity.
It is made available under a CC-BY-NC-ND 4.0 International license .

Introduction

Autism spectrum disorder (referred to as "autism" hereafter) affects approximately 1% of children around the world[1] and is characterized by difficulties with social communication and interaction, restricted and repetitive behaviors, and sensory atypicalities[2]. There is a need to better appreciate the neurobiological correlates of autistic traits in youth, which will help improve understanding of the condition and might aid potential clinical utility. Furthermore, there is a growing movement to characterize conditions like autism along dimensions of function[3-7].

There are numerous approaches to characterize the brain-based correlates of autism traits using functional magnetic resonance imaging (fMRI) connectivity data, in which measures of similarity of the blood-oxygen-level-dependent (BOLD) signal are computed between different regions of interest[8]. In particular, prediction-based studies—using functional connectivity data to predict a phenotype—have proven promising. For instance, case-control studies have focused on classifying those with autism compared to neurotypical participants, showing that high prediction accuracy can be achieved on the basis of functional connectivity differences[9-18]. Another approach predicts continuous measures of a phenotype (a symptom scale or a behavioral test score)[18-21]. One method of dimensional prediction is connectome-based predictive modelling (CPM)[22,23], which seeks to identify the functional connections most strongly predictive of a given phenotype. Groups using CPM in autism samples have identified brain-behavior correlates of clinician-rated autism symptoms[24,25], and other traits, such as behavioral inhibition[26], social responsiveness[24,27], and attentional states[28].

Nevertheless, which conditions yield the best predictive modeling performance is still largely understudied. Most studies have typically focused on resting-state fMRI, in which

medRxiv preprint doi: https://doi.org/10.1101/2025.01.14.24319457; this version posted January 17, 2025. The copyright holder for this preprint (which was not certified by peer review) is the author/funder, who has granted medRxiv a license to display the preprint in perpetuity.
It is made available under a CC-BY-NC-ND 4.0 International license .

participants rest quietly in the scanner. However, in neurotypical participants, the importance of scanning condition (e.g., 'brain state') is being recognized[29-32] for prediction of various phenotypes, including intelligence[33-35], attention[36,37], working memory[38,39], personality traits[40], cognition and emotion scores[41], as well as for emphasizing individual differences in connectivity patterns[42]. These studies suggest that predicting out-of-scanner phenotypes using connectivity measured during task performance tend to increase prediction accuracy particularly when the task probes some aspect of the out-of-scanner item of interest (e.g., memory tasks in the scanner tend to result in higher prediction of memory performance outside the scanner[38]).

In addition, there are a number of elegant studies showing that in-scanner attention tasks can be used to inform the neurobiological organization of autism[43-47]. There are also other brain imaging studies suggesting an overlap between the functional networks mediating ADHD and autism[24,48]. At a behavioral level, the co-occurrence of autism and attention-deficit/hyperactivity disorder (ADHD) symptoms has long been acknowledged[49-52].

Motivated by the importance of tasks in assessing phenotypes, as well as the importance of attention in autism, here we consider brain state-associated improvements in prediction performance in a sample of youth with autism and neurotypical participants. Using data from three different scanning conditions—a task requiring sustained attention, a task requiring selective social attention (SSA), and resting-state data—we applied CPM to probe brain-behavior relationships. Specifically, the gradual onset continuous performance task (gradCPT)[36,53,54] tests the ability to sustain attention to constantly changing stimuli. The SSA task captures ability to process dynamic, multimodal faces within a complex visual scene, which represents one of the best replicated eye-tracking biomarkers in autism[55-59]. The task was designed such that speech

medRxiv preprint doi: https://doi.org/10.1101/2025.01.14.24319457; this version posted January 17, 2025. The copyright holder for this preprint (which was not certified by peer review) is the author/funder, who has granted medRxiv a license to display the preprint in perpetuity.
It is made available under a CC-BY-NC-ND 4.0 International license .

(SP) and eye contact (EC) were varied, allowing us to assess the effect of each condition on prediction performance.

We hypothesized that consistent with the social features of autism, prediction performance of autistic traits would be highest in the SSA task and would increase with the presence of increased social cues. Specifically, we expected that the condition containing both eye contact and speech (EC+SP+) would yield the strongest prediction performance. We hypothesized that the next highest prediction performance would result from the sustained attention task, due to the restricted and repetitive behaviors observed in autism, and that both tasks would outperform resting-state data. To determine if results were robust, we used two other datasets to determine if successful models can generalize to external samples. One of the datasets was used to assess the model's generalizability in predicting performance on an attention task; the other dataset was used to assess prediction of other autistic features.

Results

Overview

Three samples were used in this work (Figure 1). The first dataset comprised 63 subjects from a sample described previously (mean age = 11.7 years, st. dev. = 2.8 years; 29 females; mean IQ = 107.8, st. dev. = 15.1)[28,60]. Twenty participants had autism; 11 other participants had a neurodevelopmental condition (five had attention-deficit/hyperactivity disorder (ADHD), two had anxiety disorder, and four were classified as belonging to the broader autism phenotype)[61]. Hereafter, we refer to this dataset as the "Yale youth sample." Autism symptoms were scored using the Autism Diagnostic Observation Schedule-2 (ADOS-2)[62].

medRxiv preprint doi: https://doi.org/10.1101/2025.01.14.24319457; this version posted January 17, 2025. The copyright holder for this preprint (which was not certified by peer review) is the author/funder, who has granted medRxiv a license to display the preprint in perpetuity.
It is made available under a CC-BY-NC-ND 4.0 International license .

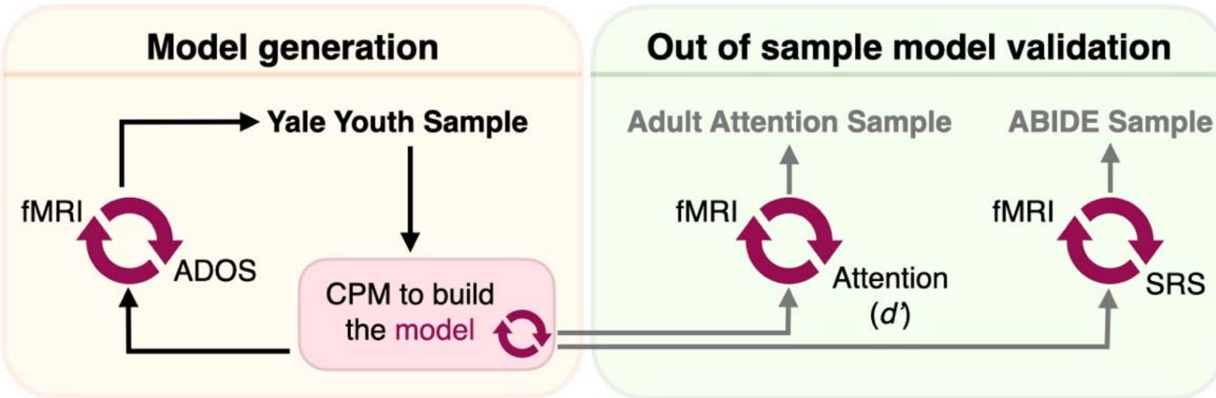

Figure 1. An overview of the datasets used in this study. The Yale youth sample was the first dataset used. FMRI connectivity data from different scanning conditions (task and rest) were used to generate connectome-based predictive models of Autism Diagnostic Observation Schedule (ADOS) scores (red circular arrows denote a brain-behavior predictive model). A summary predictive model was then generated and applied to the adult attention sample. The goal of this step was to determine whether the model generalized to predict attention phenotypes (*d*') in an external dataset. The summary model was also applied to ABIDE to determine if the model predicted SRS scores in an external sample. ABIDE, autism brain imaging data exchange; ADOS, Autism Diagnostic Observation Schedule; CPM, connectome-based predictive model; *d*', d-prime (attention phenotype in the Adult Attention Sample); SRS, social responsiveness scale.

Participants in the Yale youth sample completed three different scanning conditions (Figure 2; see Methods for further description of each task). We note that the SSA clips were counterbalanced across participants; the other scan conditions were not (Supplemental Materials; Supplemental Figure 1). A standard preprocessing approach was used to generate connectomes[33,63-65] from the different scanning conditions using a 268-node atlas[22]. For each subject, the mean time-course of each region of interest ("node" in graph theory) was computed, and the Pearson correlation coefficient was calculated between each pair of nodes to achieve a symmetric 268 x 268 matrix of correlation values representing "edges" (connections between nodes) in graph theory. The Pearson correlation coefficients were then transformed to *z*-scores via a Fisher transformation, and only the upper triangle of the matrix was considered, yielding 35,778 unique edges.

medRxiv preprint doi: https://doi.org/10.1101/2025.01.14.24319457; this version posted January 17, 2025. The copyright holder for this preprint (which was not certified by peer review) is the author/funder, who has granted medRxiv a license to display the preprint in perpetuity.
It is made available under a CC-BY-NC-ND 4.0 International license .

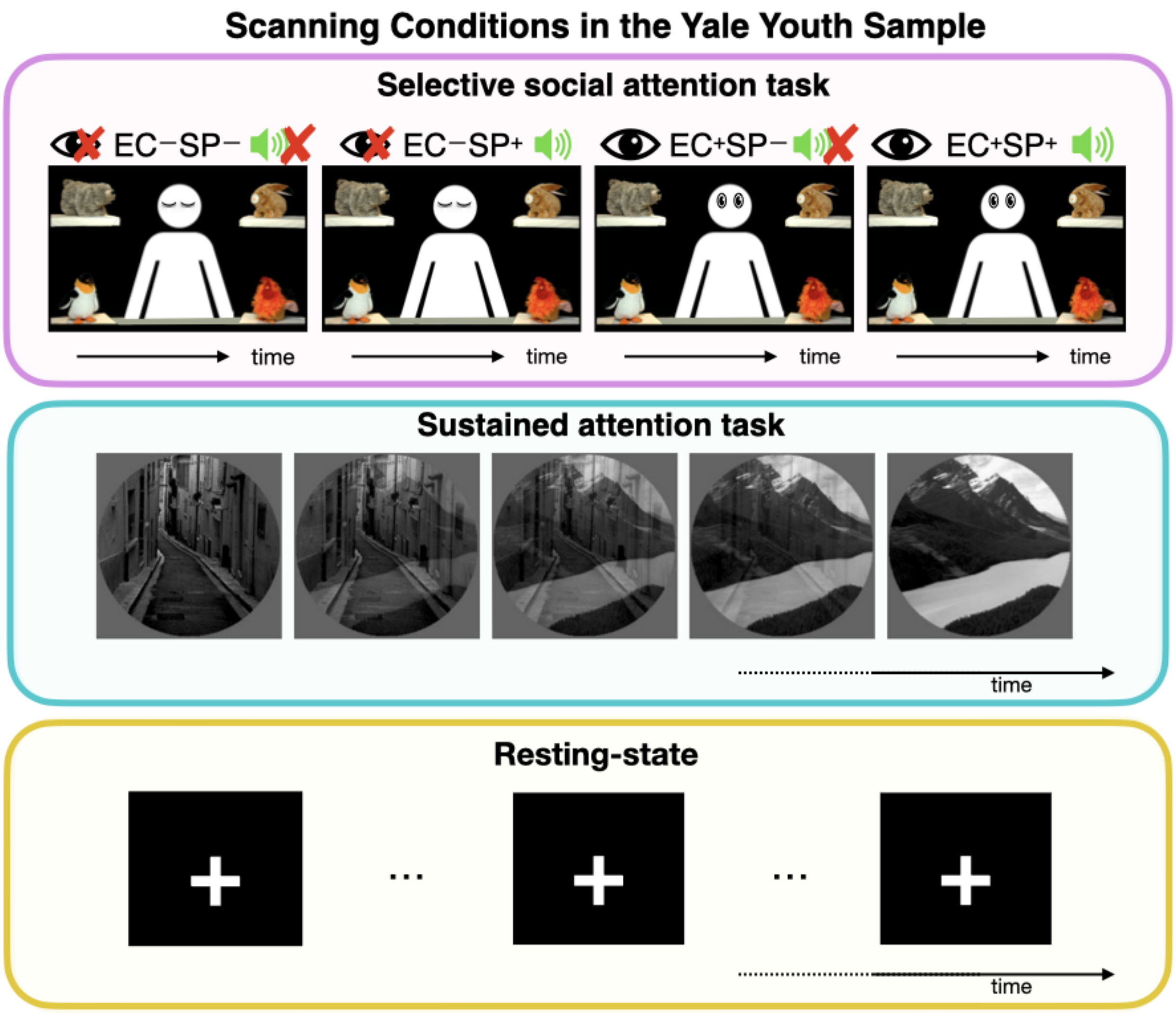

Figure 2. A schematic showing the scanning conditions used in the Yale youth sample. Top panel: free-viewing selective social attention task. Four conditions were shown to participants: no eye contact, no speech (EC-SP-); no eye contact, with speech (EC-SP+); eye contact, with no speech (EC+SP-); and eye contact, with speech (EC+SP+). Note we have obscured the actress in the preprint version for confidentiality. Middle panel: the gradual onset continuous performance task (gradCPT) was used as a sustained attention task. Grayscale pictures of cities and mountains were presented with images gradually transitioning from one to the next; button presses were required for city scenes and withheld for mountain scenes. Bottom panel: resting-state condition, in which the participants viewed a fixation cross. Please see the Methods section for further details about each scanning condition.

<u>Prediction performance is highest in the Yale youth sample using task data</u>

We first assessed which scanning condition resulted in the highest prediction performance of autistic traits in the Yale youth sample. To ensure consistent amounts of data

medRxiv preprint doi: https://doi.org/10.1101/2025.01.14.24319457; this version posted January 17, 2025. The copyright holder for this preprint (which was not certified by peer review) is the author/funder, who has granted medRxiv a license to display the preprint in perpetuity.
It is made available under a CC-BY-NC-ND 4.0 International license .

across scanning conditions, we discarded frames from the end of gradCPT and resting-state runs, such that the total amount of data was the same as from the Selective Social Attention task runs (four minutes of data). CPM[23] was then used to assess prediction performance of ADOS scores (Supplemental Figure 2) and was repeated 500 times. Head motion was controlled for during CPM as before[28,66,67]. The median performing model is represented in the text below, as well as prediction ranges where appropriate; significance was assessed via permutation testing (Methods).

We found differential performance across the various task conditions (Figure 3; Supplemental Table 1). For example, performance using the resting-state data was quite low (rest 1, Spearman’s rho = 0.093, *P*-value = 0.115; rest 2, Spearman’s rho = 0.18, *P*-value = 0.062), and prediction performance was noted to have substantial variance (i.e., using data from resting-state run 1, the minimum Spearman's rho = -0.2017, maximum Spearman's rho = 0.337, with 15% of the prediction performance scores below zero). Performance was also quite low in the SSA condition with no eye contact and no speech (EC-SP-; Spearman’s rho = -0.106, *P*-value = 0.41). Surprisingly, there was large variance in prediction performance scores using the SSA condition with eye contact and speech (EC+SP+; minimum Spearman’s rho = -0.172; maximum Spearman’s rho = 0.323, with 7.2% of the prediction performance scores below zero). Prediction performance was higher in the other SSA conditions, but was not statistically significant after correcting for multiple comparisons (EC+SP-: Spearman’s rho = 0.251, *P*-value = 0.026; EC-SP+: Spearman’s rho = 0.266, *P*-value = 0.017). The only condition that resulted in statistically significant brain-behavior predictions was gradCPT 1 (Spearman’s rho = 0.441, *P*-value = 0.002, corrected). See Supplemental Table 1 for statistics for all CPM analyses.

medRxiv preprint doi: https://doi.org/10.1101/2025.01.14.24319457; this version posted January 17, 2025. The copyright holder for this preprint (which was not certified by peer review) is the author/funder, who has granted medRxiv a license to display the preprint in perpetuity.
It is made available under a CC-BY-NC-ND 4.0 International license .

Prediction performance has been noted to increase with increasing amounts of data[68], possibly due to an increase in reliability of functional connectivity estimates[69-71]. We tested this possibility by combining data from gradCPT 1 and gradCPT 2, as well as resting-state session 1 and resting-state session 2. More data led to a slight increase in prediction performance using both gradCPT and rest (Figure 3), though only gradCPT prediction performance was statistically significant after multiple comparisons correction (gradCPT average: Spearman's rho = 0.445, *P*-value = 0.001, corrected; rest average: Spearman's rho = 0.296, *P*-value = 0.019).

To ensure results were internally consistent, we repeated the CPM analysis using a multiverse approach, which assesses how results are affected by different analytical choices[72]. The point of this approach is not to determine what CPM pipeline results in the highest prediction performance. Instead, the goal is to assess various analytical scenarios and determine how arbitrary modelling choices impact CPM performance. In the Yale youth sample, we first adjusted CPM models for age, sex, and IQ. Encouragingly, we found similar results to that above: gradCPT results in the highest prediction performance; the SSA task with no eye contact and no speech results in the lowest (Supplemental Table 2). The other SSA task conditions did not tend to result in high predictions; rest performance was also low.

We continued with the multiverse analysis and repeated CPM using the same pipeline as above, except instead of predicting total ADOS scores, we attempted to predict the social affect and the restricted and repetitive behaviors subscales of the ADOS. We observed the same overall trend—gradCPT tends to result in the highest prediction performance and the resting-state and SSA task with no eye contact and no speech performed the poorest (Supplemental Figure 3; Supplemental Table 1). Interestingly, the SSA tasks resulted in

medRxiv preprint doi: https://doi.org/10.1101/2025.01.14.24319457; this version posted January 17, 2025. The copyright holder for this preprint (which was not certified by peer review) is the author/funder, who has granted medRxiv a license to display the preprint in perpetuity.
It is made available under a CC-BY-NC-ND 4.0 International license .

increased prediction performance of social affect scores, but predictions were not significant after controlling for multiple comparisons. Prediction performance of restricted and repetitive behaviors using the SSA data tended to be low. (Note that we continued with the multiverse approach below when assessing generalizability; see ‘Testing generalizability of the ADOS network’ in the Methods for a full description of all parameters tested in the multiverse analysis.)

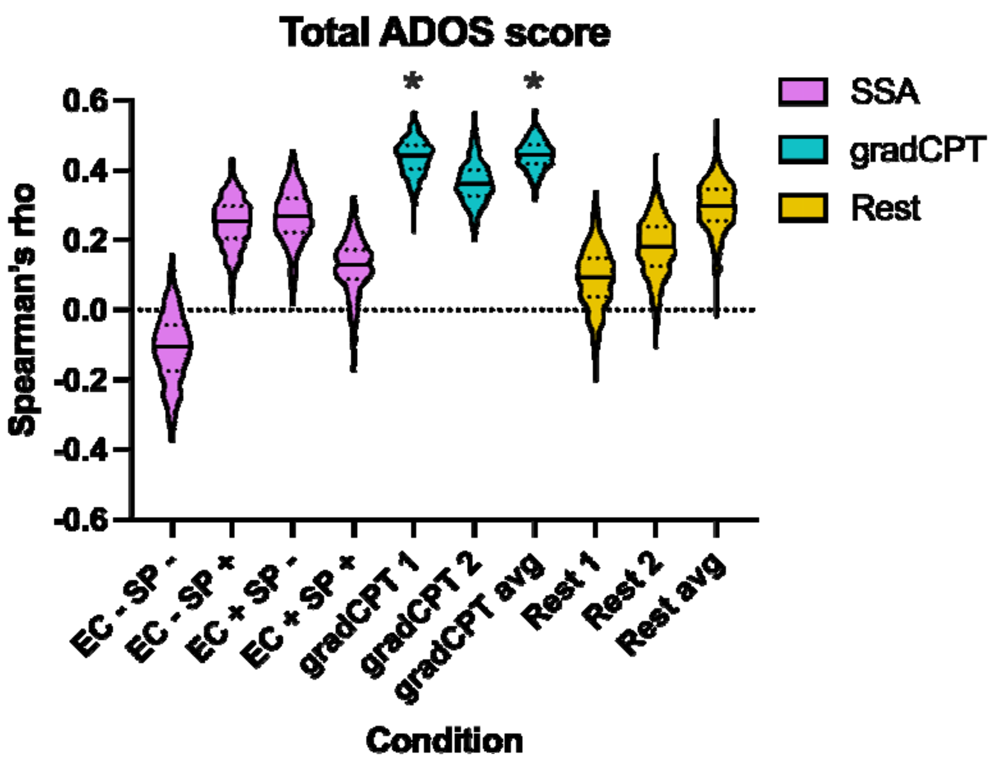

Figure 3. CPM prediction performance across different scanning conditions for total ADOS scores. The scan condition is shown on the x-axis; on the y-axis, Spearman’s rho is shown for the correlation of predicted and actual ADOS scores. For each condition, the median of the 500 iterations is shown as a solid black line in the violin plot; quartiles, as dotted lines. The Selective Social Attention task conditions are shown in purple, gradCPT in turquoise, and resting-state data in yellow. Asterisk (*) indicates statistical significance after correcting for multiple comparisons. ADOS, autism diagnostic observation schedule; Avg, average; EC-SP-, no eye contact, no speech; EC-SP+, no eye contact, with speech; EC+SP-, eye contact, with no speech; EC+SP+, eye contact, with speech; mm, millimeters; SSA, selective social attention task.

medRxiv preprint doi: https://doi.org/10.1101/2025.01.14.24319457; this version posted January 17, 2025. The copyright holder for this preprint (which was not certified by peer review) is the author/funder, who has granted medRxiv a license to display the preprint in perpetuity.
It is made available under a CC-BY-NC-ND 4.0 International license .

External validation of predictive models—attention prediction in the adult attention sample

Having determined that data derived from attention tasks are best for predicting autistic traits, we next assessed generalizability of the attention predictive model. Previously, we have shown it is possible to build predictive models of sustained attention in the Yale youth sample and that such a model is related to autistic traits[28]. Therefore, we assessed the extent to which predictive models of autistic traits are related to sustained attention. To ensure generalizability was not driven by sample-specific noise, we tested the predictive model in an external dataset of individuals performing the same gradCPT task (n=25 neurotypical adults, 13 females, mean age = 22.8 years, st. dev. = 3.5 years)[36]. Hereafter, we refer to this dataset as the “adult attention sample” (Figure 1). The behavioral outcome of interest in this sample is performance on the gradCPT, *d’* (sensitivity), the participant’s hit rate minus false alarm rate (mean *d*’ = 2.11, st. dev. = 0.92).

We determined which edges tended to contribute consistently to successful prediction of ADOS phenotypes in the Yale youth sample (see Methods, ‘Testing generalizability of the ADOS network’) using the model generated from average gradCPT data in the prediction of total ADOS scores. The resulting model (the ‘ADOS consensus network’) was used to determine if there was a relationship between predicted ADOS scores and *d*’ scores in the adult attention sample. Specifically, we used the fMRI gradCPT task data from the adult attention sample to generate a predicted ADOS score. Predicted ADOS scores were then compared to actual *d*’ scores across participants to assess accuracy. We point out this differs from the Yale youth sample, where we were able to compare predicted ADOS scores with

medRxiv preprint doi: https://doi.org/10.1101/2025.01.14.24319457; this version posted January 17, 2025. The copyright holder for this preprint (which was not certified by peer review) is the author/funder, who has granted medRxiv a license to display the preprint in perpetuity.
It is made available under a CC-BY-NC-ND 4.0 International license .

observed ADOS scores. In the adult attention sample, the goal was to assess the relationship between the model (trained to predict ADOS) and attention (*d*').

We observed a statistically significant relationship between predicted ADOS scores and *d*' scores (Spearman's rho = -0.56, *P* = 0.0049, corrected; Figure 4A). Specifically, higher predicted ADOS scores were associated with lower *d*' scores, indicating poorer performance on the task and implying lower sustained attention. To ensure results were robust, we repeated analyses controlling for potential confounds; predictions remained high when adjusting for participant head motion (Spearman's rho = -0.56, *P* = 0.0043), participant sex (Spearman's rho = -0.49, *P* = 0.0164), and participant age (Spearman's rho = -0.55, *P* = 0.0066). In addition, we also assessed the relationship between predicted ADOS scores and *d*' scores using only the ADOS positive network and then only the ADOS negative network. We observed a statistically significant negative correlation in the ADOS positive model (Spearman's rho = -0.59, *P* = 0.0021, corrected; Figure 4B) and in the ADOS negative model (Spearman's rho = -0.46, *P* = 0.023, corrected; Figure 4C).

We also calculated combined network strength in the consensus networks and computed correlations (Spearman) with *d*' in the adult attention sample. A statistically significant relationship was observed between ADOS network strength and *d*' score (Spearman's rho = -0.58, *P* = 0.002, corrected; Supplemental Figure 4A). Specifically, higher network strength in the ADOS network is associated with a lower *d*' score, indicating poorer performance on the task. In addition, a statistically significant negative correlation was also observed in the ADOS positive model (Spearman's rho = -0.62, *P* = 0.001, corrected; Supplemental Figure 4B) and a positive correlation in the ADOS negative model (Spearman's rho = 0.50, *P* =

medRxiv preprint doi: https://doi.org/10.1101/2025.01.14.24319457; this version posted January 17, 2025. The copyright holder for this preprint (which was not certified by peer review) is the author/funder, who has granted medRxiv a license to display the preprint in perpetuity.
It is made available under a CC-BY-NC-ND 4.0 International license .

0.011, corrected; Supplemental Figure 4C), confirming that connectivity strength in the consensus networks aligns with *d'* in the expected directions.

Lastly, we altered the stringency of how often an edge had to be included in the ADOS consensus model (Methods). We observed consistent results across a range of thresholds (Supplemental Table 3), increasing confidence that there is a relationship between ADOS network strength and *d'* scores. In sum, these results suggest that the predictive model of autistic traits captures variance related to sustained attention.

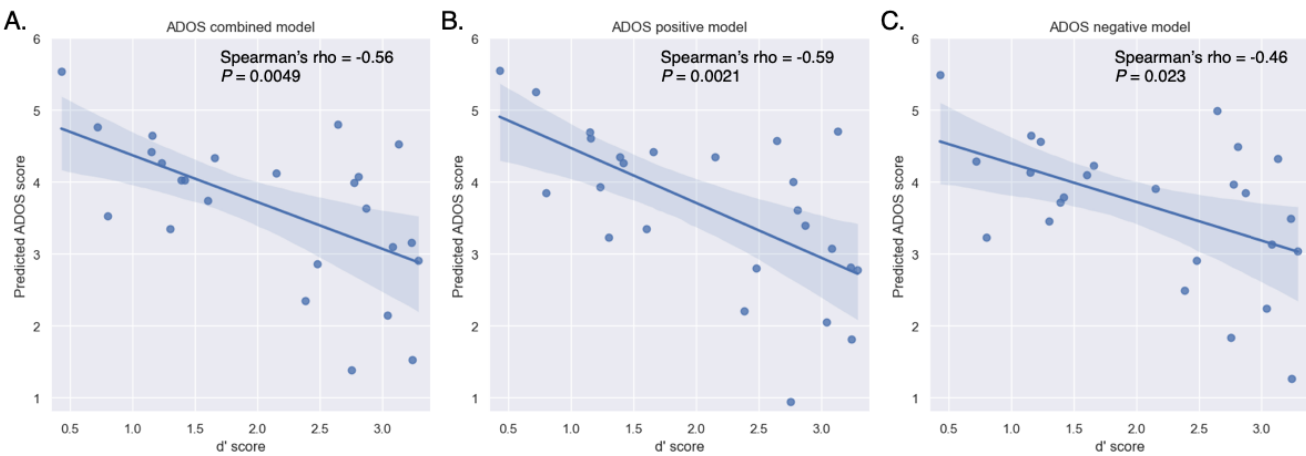

Figure 4. Generalization of the ADOS consensus network in the adult attention sample. A. Results using the combined network model. B. Results using the positive-association network model. C. Results using the negative-association network model. Predicted ADOS scores are indicated on the *y*-axis; *d'* scores, on the *x*-axis. Higher predicted ADOS scores are associated with lower *d'* scores, indicating poorer performance on the task and implying lower sustained attention. A regression line and 95% confidence interval are shown. ADOS, autism diagnostic observation schedule; *P*□=□*P*-value.

External validation of predictive models—social responsiveness prediction in ABIDE

After finding we could successfully predict attention scores, we set out to determine if the predictive model from the Yale youth sample generalized to predict social responsiveness in a large sample of participants from ABIDE (n=229, 65 females; mean age = 10.45 years, st.

medRxiv preprint doi: https://doi.org/10.1101/2025.01.14.24319457; this version posted January 17, 2025. The copyright holder for this preprint (which was not certified by peer review) is the author/funder, who has granted medRxiv a license to display the preprint in perpetuity.
It is made available under a CC-BY-NC-ND 4.0 International license .

dev. = 1.8 years; mean IQ = 113.7, st. dev. = 15.1)[73,74] described previously[24]. We used the same approach as in the adult attention sample to assess generalizability. Specifically, we used the resting-state data from ABIDE and applied the ADOS consensus model to predict social responsiveness scale (SRS) scores[75] across participants (Methods). As with the other test of generalizability above, predicted ADOS scores were then compared to actual SRS scores to assess accuracy.

We observed successful prediction of all SRS scales tested (Figure 5). In particular, the model generalized to predict SRS total scores (Spearman's rho = 0.17, P = 0.008, corrected, Figure 5A), as well as SRS subscales quantifying communication (Spearman's rho = 0.15, P = 0.028, corrected, Figure 5B), mannerisms (Spearman's rho = 0.21, P = 0.001, corrected, Figure 5C), and motivation (Spearman's rho = 0.16, P = 0.016, corrected, Figure 5D). We also tested prediction of each SRS scale after adjusting for participant age, sex, and head motion; predictions were essentially unchanged, further supporting that the ADOS model is capturing variance related to the SRS scales (Supplemental Table 4).

As above, we altered how often an edge had to be included in the ADOS CPM and retested predictions. In every case, we observed similar predictions across various thresholds for all SRS scales (Supplemental Table 5). Taken together, these data indicate the ADOS model from the Yale youth sample generalizes to predict aspects of sociality in ABIDE.

medRxiv preprint doi: https://doi.org/10.1101/2025.01.14.24319457; this version posted January 17, 2025. The copyright holder for this preprint (which was not certified by peer review) is the author/funder, who has granted medRxiv a license to display the preprint in perpetuity.
It is made available under a CC-BY-NC-ND 4.0 International license .

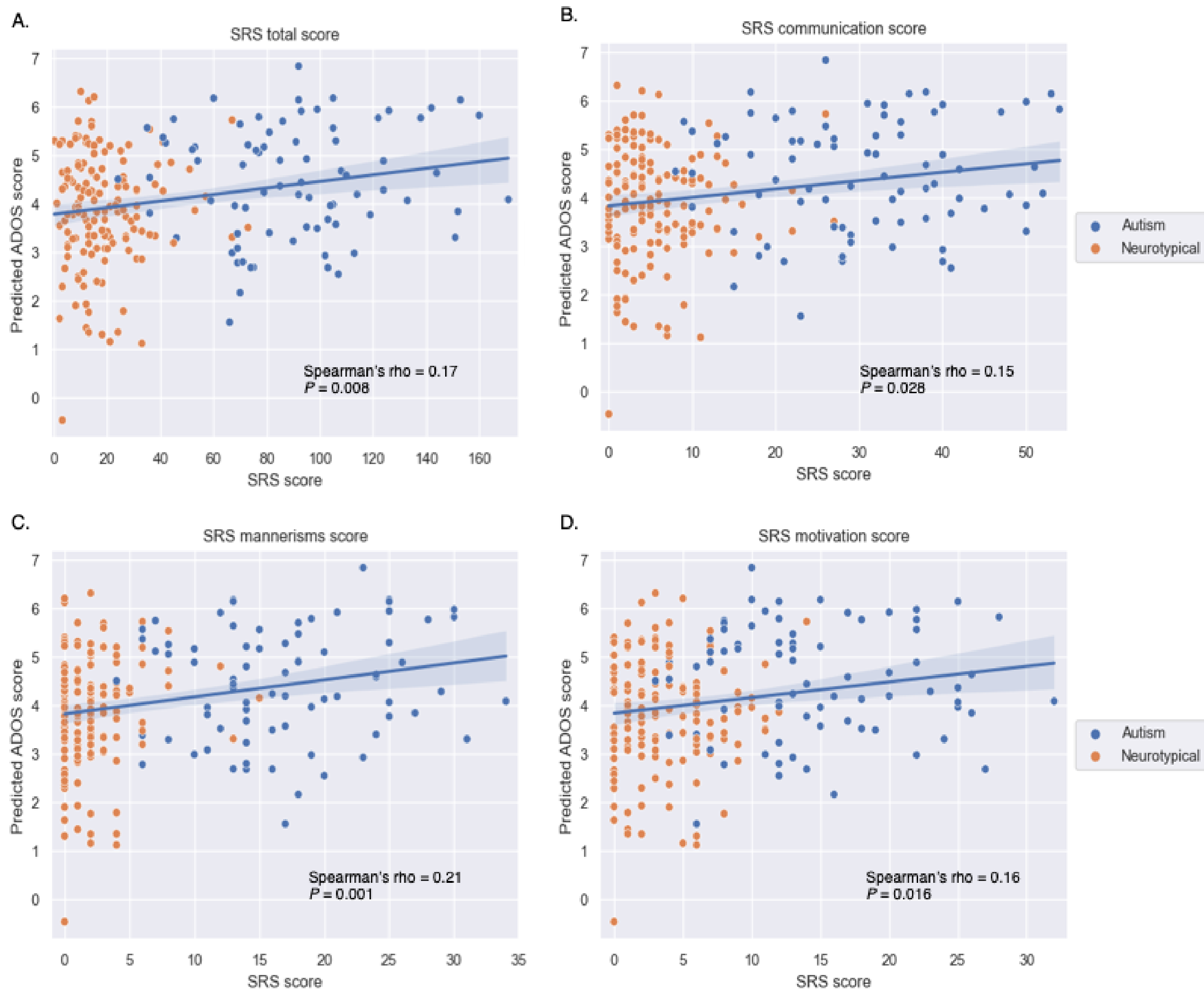

Figure 5. Generalization of the ADOS consensus network to ABIDE. A. SRS total score results. B. SRS communication score results. C. SRS mannerism score results. D. SRS motivation score results. For all plots, actual SRS scores from each subscale are indicated on the *x*-axis; predicted scores, on the *y*-axis. A regression line and 95% confidence interval are shown. ADOS, autism diagnostic observation schedule; *P* = *P*-value; SRS, social responsive scale.

Neuroanatomy of predictive edges

Finally, we visualized brain connections in the ADOS consensus model. The network comprised 2,014 total edges (1,001 edges in the positive-association and 1,013 edges in the negative-association network), approximately 5.6% of the connectome. Edges across the brain

medRxiv preprint doi: https://doi.org/10.1101/2025.01.14.24319457; this version posted January 17, 2025. The copyright holder for this preprint (which was not certified by peer review) is the author/funder, who has granted medRxiv a license to display the preprint in perpetuity.
It is made available under a CC-BY-NC-ND 4.0 International license .

were represented in the model, constituting a complex, distributed network (Figure 6A-B). In particular, connections within and between heteromodal association networks were found to contain the highest fraction of edges (Figure 6C-D; note that results have been corrected for differing network size)[28]. For instance, the top three network pairs containing the greatest proportion of edges in the positive-association network involved medial frontal, frontoparietal, or default mode networks. In the negative-association network, the top three network pairs involved connections within and between medial frontal, frontoparietal, or default mode networks (e.g., in this case, the top network pair comprised connections within the medial frontal network; the next highest network comprised connections between the medial frontal and frontoparietal networks; and the third highest network connected the medial frontal and default mode networks). In addition, 704/1001 of the edges in the positive-association network and 535/1013 of the edges connected to medial frontal, frontoparietal, or default mode networks. We performed further visualizations using slightly different thresholding techniques; these analyses again showed that association networks were important in the ADOS consensus model (Supplemental Figure 5).

medRxiv preprint doi: https://doi.org/10.1101/2025.01.14.24319457; this version posted January 17, 2025. The copyright holder for this preprint (which was not certified by peer review) is the author/funder, who has granted medRxiv a license to display the preprint in perpetuity.
It is made available under a CC-BY-NC-ND 4.0 International license .

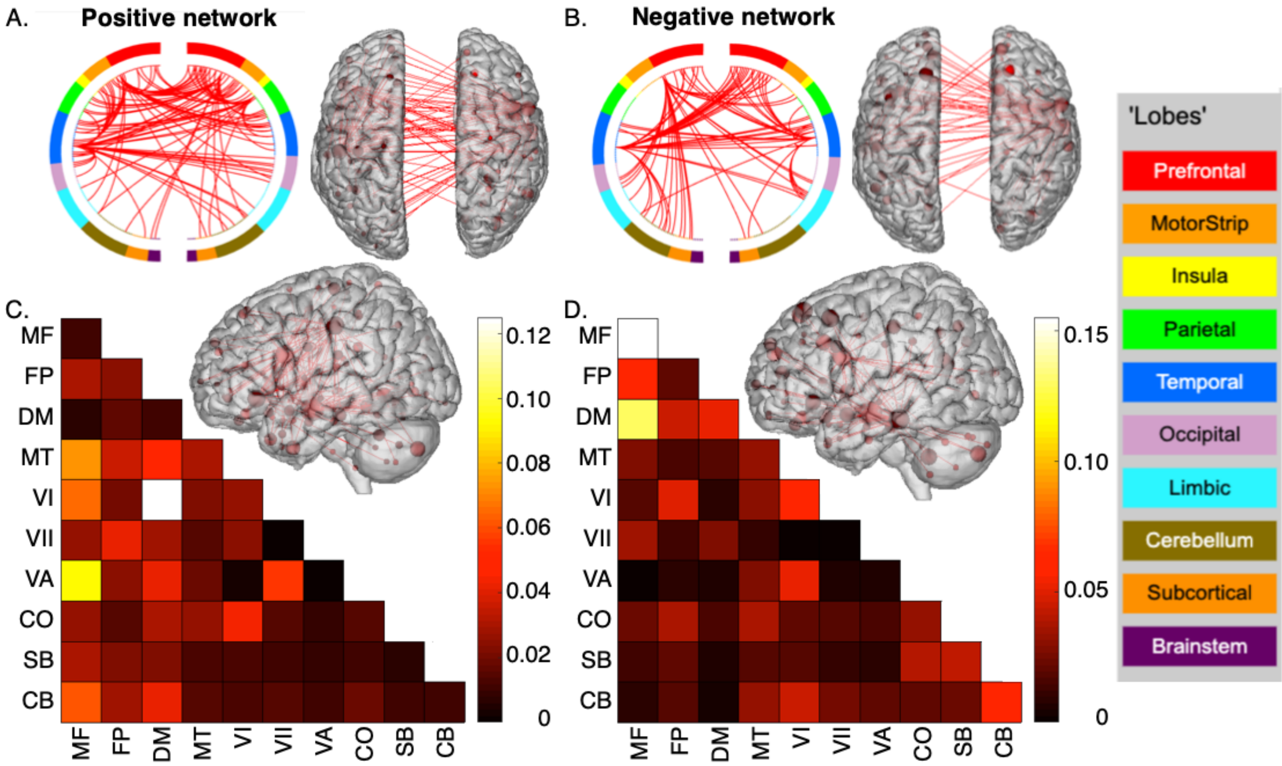

Figure 6. Neuroanatomy of ADOS consensus network. A. The positive-association network. B. The negative-association network. For both A and B: a circle plot is shown in the upper left. The top of the circle represents anterior; the bottom, posterior. The left half of the circle plot corresponds to the left hemisphere of the brain. A legend indicating the approximate anatomic 'lobe' is shown to the left. The same edges are plotted in the glass brains as lines connecting different nodes (red circles); in these visualizations, nodes are sized according to degree, the number of edges connected to that node. To aid in visualization, we have thresholded the matrices to only show nodes with a degree threshold > 25. C. Matrix of the positive-association network. D. Matrix of the negative-association network. For both C and D: The proportion of edges in a given network pair is shown; data have been corrected to account for differing network size. MF, medial frontal; FP, frontoparietal; DM, default mode; MT, motor; VI, visual I; VII, visual II; VA, visual association; CO, cingulo-opercular; SB, subcortical; CB, cerebellum.

Discussion

We determined that using functional connectivity calculated from data acquired during gradCPT resulted in the prediction of autistic traits and generalized to independent samples to predict attention and social phenotypes in neurotypical participants and those with autism.

medRxiv preprint doi: https://doi.org/10.1101/2025.01.14.24319457; this version posted January 17, 2025. The copyright holder for this preprint (which was not certified by peer review) is the author/funder, who has granted medRxiv a license to display the preprint in perpetuity.
It is made available under a CC-BY-NC-ND 4.0 International license .

Altogether, results highlight the potential of using in-scanner tasks, particularly those demanding sustained attention, to more accurately determine brain-behavior relationships in clinical samples.

There is a rich history of using tasks to probe the cognitive architecture of autism[76-81]. Nevertheless, most fMRI brain-behavior prediction studies in autism that use machine learning techniques have typically relied on resting-state data (see[4] for a recent review). Our results suggest that by optimizing the brain state under which data are acquired through task engagement[82], more accurate brain-behavior relationships can be studied[29]. Improved brain-behavior mapping increases the potential clinical utility of neuroimaging approaches[83] and might help obtain a more accurate picture of brain circuits underlying the complex phenotypic landscape of autism. Tasks also offer the advantage of improving the reliability of task-engaged functional connections[84]. More generally, the results obtained here are in line with other work in neurotypical populations indicating that predictions of phenotypes improve when using task as opposed to resting-state data[29,33,34,36,41,85,86]. We note that resting-state studies still retain utility, particularly in terms of ease of data collection and their ability to facilitate the collation of large datasets across centers.

Our work adds to the growing literature suggesting an important link between autism and attention, at both neurobiological and phenotypic levels. Previous studies[24,47,87,88] have indicated that complex models spanning numerous functional networks are important for attention in autism, particularly in higher order resting-state networks, such as the default mode network (recently reviewed in[89]). Hence, the ADOS consensus model continues to highlight the role of the default mode network in mediating attention related to autistic traits. In addition, attention has been posited as playing a key role in the central behavioral manifestations of autism[90].

medRxiv preprint doi: https://doi.org/10.1101/2025.01.14.24319457; this version posted January 17, 2025. The copyright holder for this preprint (which was not certified by peer review) is the author/funder, who has granted medRxiv a license to display the preprint in perpetuity.
It is made available under a CC-BY-NC-ND 4.0 International license .

Broadly considered, attention is the means by which information is selectively perceived. It makes sense that some of the core features of autism—restricted and repetitive behaviors and social abilities—depend intimately on a process governing how external stimuli gain access to an individual's internal world. Indeed, the co-occurrence of autism and ADHD symptoms has long been acknowledged[49-51,91].

It is perhaps surprising that the SSA clips did not result in higher prediction performance. One explanation is that the SSA clips resembled resting-state[92], in that they were passive experiences in which participants could essentially attend to whatever they wanted[55,56]. It has been noted that the unconstrained nature of the resting-state is suboptimal for probing certain aspects of brain-behavior relationships[29]. Similarly, it is also perhaps surprising that the gradCPT data resulted in the highest prediction performance. Beyond attention, the highly structured, rules-based design of gradCPT may effectively highlight variations in networks linked to autistic traits, given the rules-based tendencies observed in autism[93].

In addition, it must be noted that the SSA task and resting-state conditions might have underperformed with respect to prediction performance as they came later in the study (i.e. following gradCPT) and participants were possibly fatigued. Nevertheless, previous work has shown that arousal does not appear to drive differences in predictions across different scanning conditions and that increased prediction performance seems to be due to cognitive differences driven by the task[41]. Future work could more fully investigate the role of arousal in brain-behavioral relationships in autism, while accounting for the challenging realities of scanning youth with neurodevelopmental conditions. (See Supplemental Methods for more about task design choices in the current study.)

medRxiv preprint doi: https://doi.org/10.1101/2025.01.14.24319457; this version posted January 17, 2025. The copyright holder for this preprint (which was not certified by peer review) is the author/funder, who has granted medRxiv a license to display the preprint in perpetuity.
It is made available under a CC-BY-NC-ND 4.0 International license .

These findings underscore the importance of considering both practical and conceptual aspects of task design—both the study population and the nuts and bolts of collecting high quality data must be considered when planning an fMRI study[94]. Further, other populations that are difficult to study and/or tend to exhibit significant head motion, like those with schizophrenia[95] or bipolar disorder[96], could have study designs optimized from both conceptual and practical standpoints. In some cases, demanding tasks requiring participants to be actively engaged might be desired. In other cases, more passive designs, like age-appropriate, naturalistic movie clips[97,98], might be better suited. In yet other cases, resting-state data may be collected and meaningfully linked to behavior[99,100].

In this work, we attempted to balance a 'deep' approach, which involves collecting many scans from the same subject[101], with a 'broad' approach, which involves collecting data from many subjects[102,103]. Hence, the data allowed us to compare the conditions across subjects, though this necessarily limited our sample size. Additionally, acquiring high-quality data from youth with autism is often time-intensive. In our experience, it is necessary to conduct a mock scan for at least an hour to adequately prepare a participant for the scanning environment[60]. The time commitment is on par with that reported by other groups in youth with neurodiverse conditions[104,105].

In our view, investing such time to acquire smaller samples is still necessary for the field. We contend that in the age of big data, it is essential to continue exploring brain-behavior associations in samples that might not contain thousands of subjects, but comprise unique scanning conditions. Such an approach allows the field to better determine which scans to include in big data endeavors and facilitates the exploration of questions that may be difficult to address in large-scale studies. Further, replicable and generalizable findings can still be

medRxiv preprint doi: https://doi.org/10.1101/2025.01.14.24319457; this version posted January 17, 2025. The copyright holder for this preprint (which was not certified by peer review) is the author/funder, who has granted medRxiv a license to display the preprint in perpetuity.
It is made available under a CC-BY-NC-ND 4.0 International license .

determined by using robust methods[106-108]. Collecting small, unique samples also facilitates testing across diverse experimental conditions, thereby enhancing generalizability [109]. Future work could address if findings observed here hold when sample sizes are larger.

A few final items warrant discussion. Participant IQ in the Yale youth sample and ABIDE are fairly high. More research should be conducted using participants with a broad range of IQ scores to determine which scanning conditions are optimal for prediction performance. As with other autism samples, the dataset contained mainly males; the importance of sex-based differences in brain circuitry[110-112] and behavioral phenotypes[113] relevant for autism is increasingly well-described. Finally, the current work focused on prediction of traits in an adolescent dataset. Future studies could assess task design and prediction performance in much younger samples, such as toddlers and young children. Such efforts aim to optimize the detection of brain-behavior relationships at earlier developmental stages, ultimately providing better support for individuals with autism and their families.

Conclusions

We have shown in a preliminary study that sustained attention tasks, such as gradCPT, can enhance the prediction of autistic traits. Such an approach leads to a robust marker that generalizes to predict attention and social phenotypes in independent samples. Our findings highlight the need to further investigate optimal brain states for modeling phenotypes in autism and related conditions.

Methods

Description of datasets

medRxiv preprint doi: https://doi.org/10.1101/2025.01.14.24319457; this version posted January 17, 2025. The copyright holder for this preprint (which was not certified by peer review) is the author/funder, who has granted medRxiv a license to display the preprint in perpetuity.
It is made available under a CC-BY-NC-ND 4.0 International license .

We used three datasets in this work (Figure 1). The first dataset, the Yale youth sample, comprised 63 subjects from a sample described previously (mean age = 11.7 years, st. dev. = 2.8 years; 29 females; mean IQ = 107.8, st. dev. = 15.1)[28,60]. Twenty of the participants had autism; 11 other participants had a neurodevelopmental condition (five with ADHD, two with anxiety disorder, and four were classified as belonging to the broader autism phenotype)[61]. Participants were scanned on a 3T Siemens Prisma System. See Supplementary Material for full exclusion criteria and imaging parameters. Autism symptoms were scored using the Autism Diagnostic Observation Schedule-2 (ADOS-2)[62] and were ascertained by trained clinical psychologists; calibrated severity scores were used in the present work for the social affect subscale (mean = 3.2, st. dev. = 2.9), the restricted and repetitive behavior subscale (mean = 4.0, st. dev. 3.3), and the ADOS total score (mean = 3.1, st. dev. = 3.1). This sample was used to conduct CPM, compare how scanning condition impacted performance, and generate a consensus model.

A second dataset of neurotypical adults, the adult attention sample (n=25, 13 females, mean age = 22.8 years, st. dev. = 3.5 years) was used as a validation dataset and is described elsewhere[36]. Participants were scanned on a 3T Siemens Trio TIM system. This sample was used to determine if the consensus model generalized to predict attention.

A third dataset of individuals with and without autism (n=229, 65 females; mean age = 10.45 years, st. dev. = 1.8 years; mean IQ = 113.7, st. dev. = 15.1) comprising data from ABIDE[73,74] was used as an additional validation dataset; processing of these data is described elsewhere[24]. SRS[75] scores were used from ABIDE and included the following scales: SRS total scores (mean = 42.4, st. dev. = 40.2); SRS communication (mean = 13.8, st. dev. = 14.2); SRS motivation (mean = 7.3, st. dev. = 6.9); SRS mannerisms (mean = 7.1, st. dev. = 8.5). Seventy-seven of the participants had autism. SRS was chosen due to the low numbers of subjects with

medRxiv preprint doi: https://doi.org/10.1101/2025.01.14.24319457; this version posted January 17, 2025. The copyright holder for this preprint (which was not certified by peer review) is the author/funder, who has granted medRxiv a license to display the preprint in perpetuity.
It is made available under a CC-BY-NC-ND 4.0 International license .

ADOS scores (when using the exclusion criteria described in[24]), along with the additional quality control exclusion criteria we performed (i.e., there were 229 subjects with SRS data, compared to only 33 with ADOS; see Supplemental Methods). This sample was used to determine if the consensus model generalized to predict SRS scores.

All datasets were collected in accordance with the institutional review board or research ethics committee at each site. Where appropriate, informed consent was obtained from the parents or guardians of participants. Written assent was obtained from children aged 13–17 years; verbal assent was obtained from participants under the age of 13 years.

Preprocessing of functional imaging data

A standard preprocessing approach was used that has been described elsewhere[33,63-65]. Preprocessing steps were performed using BioImage Suite[114] unless otherwise noted, and included: skull stripping the 3D magnetization prepared rapid gradient echo images using optiBET[115] and performing linear and non-linear transformations to warp a 268-node functional atlas[116] from Montreal Neurological Institute space to single subject space. Functional images were motion-corrected using SPM8 (https://www.fil.ion.ucl.ac.uk/spm/software/spm8/). Covariates of no interest were regressed from the data, including linear, quadratic, and cubic drift, a 24-parameter model of motion[117], mean cerebrospinal fluid signal, mean white matter signal, and the global signal. Data were temporally smoothed with a zero-mean unit-variance low-pass Gaussian filter (approximate cutoff frequency of 0.12 Hz). Visual inspections were performed after skull-stripping, non-linear, and linear registrations to ensure there were no errors in processing. Head motion was calculated as described previously[60] (see Supplemental Methods for additional motion control considerations, as well as Supplemental Figure 6). To ensure

medRxiv preprint doi: https://doi.org/10.1101/2025.01.14.24319457; this version posted January 17, 2025. The copyright holder for this preprint (which was not certified by peer review) is the author/funder, who has granted medRxiv a license to display the preprint in perpetuity.
It is made available under a CC-BY-NC-ND 4.0 International license .

consistent amounts of data across scanning conditions, we discarded frames from the end of the gradCPT and resting-state runs, such that the total amount of data was the same as from the SSA task runs (four minutes of data).

Connectomes were generated using a 268-node atlas[22]. For each subject, the mean time-course of each region of interest ("node" in graph theory) was computed, and the Pearson correlation coefficient was computed between each pair of nodes to achieve a symmetric 268 x 268 matrix of correlation values representing "edges" (connections between nodes) in graph theory. The Pearson correlation coefficients were then transformed to *z*-scores via a Fisher transformation, and only the upper triangle of the matrix was considered, yielding 35,778 unique edges.

Scanning conditions in the Yale Youth Sample

1) Scanning condition one: the free-viewing selective social attention task

Participants completed a novel version of a free-viewing selective social attention (SSA) task[55,58] in which an actress is presented at the center of the screen and is surrounded by objects in corners of the screen (Figure 2). Four types of clips were used in which the presence of speech (SP) and eye contact (EC) were manipulated. The first condition included clips in which the person smiled and made eye contact with the camera while speaking in full sentences (e.g., "Have you ever seen a monkey? Monkeys eat bananas, swing in trees, and chase each other."; this was designated as the EC+SP+ condition). The second condition included a direct gaze condition with no speech (EC+SP-), in which the person smiled directly at the viewer while remaining silent. The third condition consisted of the person looking down at the table while speaking in full sentences (EC-SP+). The fourth condition consisted of the person looking down

medRxiv preprint doi: https://doi.org/10.1101/2025.01.14.24319457; this version posted January 17, 2025. The copyright holder for this preprint (which was not certified by peer review) is the author/funder, who has granted medRxiv a license to display the preprint in perpetuity.
It is made available under a CC-BY-NC-ND 4.0 International license .

at the table and not speaking (EC-SP-). Each clip lasted two minutes and was shown twice over four runs, such that eight clips were shown total. To allow successful scene transitions in between sentences, the direct gaze and speech condition lasted 2 minutes and 8 seconds. The speech with no eye contact condition lasted 2 minutes and 6 seconds. In between clips during each run, a white fixation cross on a black background was shown for 15 seconds. Clip order was counterbalanced across participants (see Supplemental Materials for more about the counterbalancing of clips, as well as study design considerations of the Yale youth sample). Clip conditions were concatenated across runs, such that each resulting connectivity matrix comprised four minutes of data from a single scanning condition. Both gradCPT and the SSA task were presented using Psychtoolbox (version: 3.0.14; http://psychtoolbox.org/; MATLAB version R2018a) on a Lenovo IdeaPad 720S computer, with Ubuntu 16.04 LTS installed.

2) Scanning condition two: testing gradual onset continuous performance task (gradCPT)

The gradual onset continuous performance task (gradCPT; Figure 2) has been described previously[36,53,54]. The gradCPT tests sustained attention and inhibition, producing a range of performance scores across neurotypical[53,54] and neurodiverse populations[28]. Participants viewed grayscale pictures of cities and mountains presented at the center of the screen, with images gradually transitioning from one to the next every 1,000 ms. Subjects were instructed to respond with a button press for city scenes and to withhold button presses for mountain scenes. City scenes occurred randomly 90% of the time. Performance was calculated using *d'* (sensitivity), the participant's hit rate minus false alarm rate. The task took 5 minutes to complete; participants completed the task twice. Note that because of differences in task timing between gradCPT, the selective social attention task, and resting-state, we trimmed the gradCPT and resting-state data

medRxiv preprint doi: https://doi.org/10.1101/2025.01.14.24319457; this version posted January 17, 2025. The copyright holder for this preprint (which was not certified by peer review) is the author/funder, who has granted medRxiv a license to display the preprint in perpetuity.
It is made available under a CC-BY-NC-ND 4.0 International license .

to include 4 minutes of data per scan (to match the selective social task time length of 4 minutes).

Subjects in the adult attention sample also performed gradCPT; the same parameters were used as above, except scene transitions took 800 ms.

3) Scanning condition three: resting-state data

Resting-state data were also obtained. Subjects were instructed to keep their eyes open, relax, and think of nothing in particular while they viewed a white fixation cross on a black screen. Each scan lasted five minutes and was repeated twice per participant.

Resting-state data were also obtained in the ABIDE sample as described previously[73,74].

Connectome-based predictive modelling

CPM[23] (Supplemental Figure 1) was used to predict ADOS scores from functional connectivity data in the Yale youth sample. Briefly, using 10-fold cross-validation, connectivity matrices from a given scan condition and ADOS scores were split into an independent training set including subjects from 9 folds and a test set including the left-out fold. Linear regression was used to relate edge strength to ADOS score in the training set. Edges most strongly associated with ADOS scores were selected (feature selection threshold of $P = 0.05$) for both a 'positive network' (in which increased connectivity was associated with higher ADOS scores) and a 'negative network' (in which increased connectivity was associated with lower ADOS scores). We used partial correlation to control for mean participant head motion at the feature selection step[28,66,67]. Mean network strength was computed in both the positive and negative

medRxiv preprint doi: https://doi.org/10.1101/2025.01.14.24319457; this version posted January 17, 2025. The copyright holder for this preprint (which was not certified by peer review) is the author/funder, who has granted medRxiv a license to display the preprint in perpetuity.
It is made available under a CC-BY-NC-ND 4.0 International license .

networks, and the difference between these network strengths was computed ('combined network strength'), as in previous work [33]:

$$\text{Positive network strength}_s = \frac{1}{b}\left(\sum_{i,j} c_{i,j} {m^+}_{i,j}\right) \; ; \; b = \frac{i(j-1)}{2}$$

$$\text{Negative network strength}_s = \frac{1}{b}\left(\sum_{i,j} c_{i,j} {m^-}_{i,j}\right) ; \; b = \frac{i(j-1)}{2}$$

$$\text{Combined network strength}_s = \text{Positive network strength}_s - \text{negative network strength}_s$$

where c is the connectivity matrix for subject s and m^+ and m^- are binary matrices indexing the edges (i, j) that survived the feature selection threshold for the positive-association and negative-association networks, respectively.

A linear model was then calculated relating combined network strength to ADOS scores in the training set. In the last step, combined network strength was computed for the test set, and the model was applied to generate ADOS predictions for these unseen participants.

Model performance was assessed as reported previously [67] by comparing the similarity between predicted and observed ADOS scores using both Spearman's correlation (to avoid distribution assumptions)[118]. We performed 500 iterations of a given CPM analysis and selected the median-performing model; we report this in the main text when discussing model performance. To calculate significance, we randomly shuffled participant labels and attempted to predict ADOS scores. We repeated this 500 times and calculated the number of times a permuted predictive accuracy was greater than the median of the unpermuted predictions to achieve a non-parametric *P*-value:

$$P = (\#(\text{rho}_{\text{null}} \geq \text{rho}_{\text{median}})) / 500$$

medRxiv preprint doi: https://doi.org/10.1101/2025.01.14.24319457; this version posted January 17, 2025. The copyright holder for this preprint (which was not certified by peer review) is the author/funder, who has granted medRxiv a license to display the preprint in perpetuity.
It is made available under a CC-BY-NC-ND 4.0 International license .

where #($rho_{null} \geq rho_{median}$) indicates the number of permuted predictions numerically greater than or equal to the median of the unpermuted predictions[67]. We used the Benjamini–Hochberg method[119] to correct for multiple comparisons, correcting for ten tests in the Yale youth sample (two for gradCPT, four for SSA, two for resting-state, one for gradCPT average, and one for resting-state average), three tests in the adult attention sample, and four tests in ABIDE.

Testing generalizability of the ADOS network

To determine if the ADOS networks from the Yale youth sample generalized to external datasets (the adult attention sample and ABIDE), we defined a consensus positive-association network and consensus negative-association network as edges that appear in at least 6/10 folds in 300/500 iterations of CPM. This process resulted in 1,001 edges in the positive-association network and 1,013 edges in the negative-association network; hereafter, we refer to the collection of edges in the positive and negative networks as the 'ADOS consensus network.' We note the size of the ADOS consensus network is consistent with other CPM networks that have generalized[36,120,121]. To ensure generalizability results were robust, we tested summary networks of varying sizes (from liberal cases where an edge appeared in at least 1/10 folds and 50/500 iterations, to more stringent thresholds where an edge must appear in 10/10 folds and 500/500 iterations, moving in intervals of 1 fold and 50 iterations for each summary network).

To determine if the network predicted autistic traits, we then used the combined network strength in the ADOS consensus network and computed model coefficients across the Yale youth sample, as conducted previously[36,66,122]. Model coefficients and the network masks were

medRxiv preprint doi: https://doi.org/10.1101/2025.01.14.24319457; this version posted January 17, 2025. The copyright holder for this preprint (which was not certified by peer review) is the author/funder, who has granted medRxiv a license to display the preprint in perpetuity.
It is made available under a CC-BY-NC-ND 4.0 International license .

subsequently applied to the ABIDE sample to predict SRS scores. Model performance was determined by comparing the similarity between predicted and observed behavioral scores using Spearman's correlation. We used the same approach to determine if the network predicted *d*' scores.

To further assess generalizability, we repeated testing if the ADOS network predicts *d*' and SRS using a multiverse approach. A multiverse analysis assesses how results are affected by different analytical choices[72]. Specifically, we tested if the ADOS positive and negative networks generalized; we adjusted models for IQ, age, and sex; and, as mentioned above, we tested a range of consensus network sizes. Also, we calculated combined network strength in the consensus networks and computed correlations (Spearman) with *d*' in the adult attention sample. We performed this analysis because one could argue that in a sample of neurotypical participants, it is perhaps clinically meaningless to predict ADOS scores. We point out the goal of a multiverse approach is not to determine what pipeline results in the highest prediction performance. Instead, the point is to assess various analytical scenarios and determine how different modelling choices impact generalization. As such, we do not perform multiple comparisons correction when assessing these results.

For completeness' sake, we include the additional multiverse analyses performed in the Yale youth sample in this section. In this dataset, we adjusted CPM models for sex, age, and IQ; we also used CPM to predict social affect and restricted and repetitive behavior scores. Additionally, we assessed how altering the feature selection threshold impacted CPM. We observed a 0.01 feature selection threshold resulted in similar prediction performance using gradCPT data (data not shown), in line with previous work[28,85,122].

medRxiv preprint doi: https://doi.org/10.1101/2025.01.14.24319457; this version posted January 17, 2025. The copyright holder for this preprint (which was not certified by peer review) is the author/funder, who has granted medRxiv a license to display the preprint in perpetuity.
It is made available under a CC-BY-NC-ND 4.0 International license .

Code and data availability

Preprocessing was carried out using freely available software: (https://medicine.yale.edu/bioimaging/suite/). CPM code is freely available here: (https://github.com/YaleMRRC/CPM). The functional parcellation is available here: (https://www.nitrc.org/frs/?group_id=51). ABIDE data are available here: (https://fcon_1000.projects.nitrc.org/indi/abide/). All other data or materials are available from the authors upon request.

Acknowledgements and Disclosures

This work was supported by the National Institutes of Health (P50MH115716, T32GM007205 to CH and ASG, and TR001864 to ASG). The authors thank Hedwig Sarofin and Cheryl McMurray for assistance during the MRI sessions and Jitendra Bhawnani for assistance with hardware and software. James C. McPartland consults or has consulted with Customer Value Partners, Bridgebio, Determined Health, Apple, and BlackThorn Therapeutics, has received research funding from Janssen Research and Development, serves on the Scientific Advisory Boards of Pastorus and Modern Clinics, and receives royalties from Guilford Press, Lambert, Oxford, and Springer.

References

1 Zeidan, J. *et al.* Global prevalence of autism: A systematic review update. *Autism Res* **15**, 778-790, doi:10.1002/aur.2696 (2022).
2 American Psychiatric Association. *Diagnostic and statistical manual of mental disorders: DSM-5.* (2013).
3 Feczko, E. & Fair, D. A. Methods and Challenges for Assessing Heterogeneity. *Biol Psychiatry* **88**, 9-17, doi:10.1016/j.biopsych.2020.02.015 (2020).
4 Horien, C. *et al.* Functional Connectome-Based Predictive Modeling in Autism. *Biol Psychiatry*, doi:10.1016/j.biopsych.2022.04.008 (2022).

medRxiv preprint doi: https://doi.org/10.1101/2025.01.14.24319457; this version posted January 17, 2025. The copyright holder for this preprint (which was not certified by peer review) is the author/funder, who has granted medRxiv a license to display the preprint in perpetuity.
It is made available under a CC-BY-NC-ND 4.0 International license .

5 Insel, T. *et al.* Research Domain Criteria (RDoC): Toward a New Classification Framework for Research on Mental Disorders. *Am J Psychiat* **167**, 748-751, doi:10.1176/appi.ajp.2010.09091379 (2010).
6 Duan, X., Shan, X., Uddin, L. Q. & Chen, H. The future of disentangling the heterogeneity of autism with neuroimaging studies. *Biol Psychiatry*, doi:10.1016/j.biopsych.2024.08.008 (2024).
7 Park, S. *et al.* Delineating a Pathway for the Discovery of Functional Connectome Biomarkers of Autism. *Adv Neurobiol* **40**, 511-544, doi:10.1007/978-3-031-69491-2_18 (2024).
8 Biswal, B., Yetkin, F. Z., Haughton, V. M. & Hyde, J. S. Functional connectivity in the motor cortex of resting human brain using echo-planar MRI. *Magn Reson Med* **34**, 537-541, doi:10.1002/mrm.1910340409 (1995).
9 Anderson, J. S. *et al.* Functional connectivity magnetic resonance imaging classification of autism. *Brain* **134**, 3742-3754, doi:10.1093/brain/awr263 (2011).
10 Chen, C. P. *et al.* Diagnostic classification of intrinsic functional connectivity highlights somatosensory, default mode, and visual regions in autism. *Neuroimage Clin* **8**, 238-245, doi:10.1016/j.nicl.2015.04.002 (2015).
11 Guo, X. Y. *et al.* Diagnosing Autism Spectrum Disorder from Brain Resting-State Functional Connectivity Patterns Using a Deep Neural Network with a Novel Feature Selection Method. *Front Neurosci-Switz* **11**, doi:ARTN 460 10.3389/fnins.2017.00460 (2017).
12 Iidaka, T. Resting state functional magnetic resonance imaging and neural network classified autism and control. *Cortex* **63**, 55-67, doi:10.1016/j.cortex.2014.08.011 (2015).
13 Jahedi, A., Nasamran, C. A., Faires, B., Fan, J. & Muller, R. A. Distributed Intrinsic Functional Connectivity Patterns Predict Diagnostic Status in Large Autism Cohort. *Brain Connect* **7**, 515-525, doi:10.1089/brain.2017.0496 (2017).
14 Abraham, A. *et al.* Deriving reproducible biomarkers from multi-site resting-state data: An Autism-based example. *Neuroimage* **147**, 736-745, doi:10.1016/j.neuroimage.2016.10.045 (2017).
15 Emerson, R. W. *et al.* Functional neuroimaging of high-risk 6-month-old infants predicts a diagnosis of autism at 24 months of age. *Sci Transl Med* **9**, doi:ARTN eaag2882 10.1126/scitranslmed.aag2882 (2017).
16 Chen, H. *et al.* Multivariate classification of autism spectrum disorder using frequency-specific resting-state functional connectivity--A multi-center study. *Prog Neuropsychopharmacol Biol Psychiatry* **64**, 1-9, doi:10.1016/j.pnpbp.2015.06.014 (2016).
17 Uddin, L. Q. *et al.* Salience network-based classification and prediction of symptom severity in children with autism. *Jama Psychiat* **70**, 869-879, doi:10.1001/jamapsychiatry.2013.104 (2013).
18 Yahata, N. *et al.* A small number of abnormal brain connections predicts adult autism spectrum disorder. *Nat Commun* **7**, 11254, doi:10.1038/ncomms11254 (2016).
19 Hong, S. J. *et al.* Atypical functional connectome hierarchy in autism. *Nat Commun* **10**, 1022, doi:10.1038/s41467-019-08944-1 (2019).
20 Ilioska, I. *et al.* Connectome-wide Mega-analysis Reveals Robust Patterns of Atypical Functional Connectivity in Autism. *Biol Psychiatry* **94**, 29-39, doi:10.1016/j.biopsych.2022.12.018 (2023).

medRxiv preprint doi: https://doi.org/10.1101/2025.01.14.24319457; this version posted January 17, 2025. The copyright holder for this preprint (which was not certified by peer review) is the author/funder, who has granted medRxiv a license to display the preprint in perpetuity.
It is made available under a CC-BY-NC-ND 4.0 International license .

21 Xiao, J. *et al.* Linked Social-Communication Dimensions and Connectivity in Functional Brain Networks in Autism Spectrum Disorder. *Cereb Cortex* **31**, 3899-3910, doi:10.1093/cercor/bhab057 (2021).
22 Finn, E. S. *et al.* Functional connectome fingerprinting: identifying individuals using patterns of brain connectivity. *Nat Neurosci* **18**, 1664-1671, doi:10.1038/nn.4135 (2015).
23 Shen, X. L. *et al.* Using connectome-based predictive modeling to predict individual behavior from brain connectivity. *Nat Protoc* **12**, 506-518, doi:10.1038/nprot.2016.178 (2017).
24 Lake, E. M. R. *et al.* The Functional Brain Organization of an Individual Allows Prediction of Measures of Social Abilities Transdiagnostically in Autism and Attention-Deficit/Hyperactivity Disorder. *Biol Psychiatry* **86**, 315-326, doi:10.1016/j.biopsych.2019.02.019 (2019).
25 Ma, X. *et al.* Connectome-based prediction of the severity of autism spectrum disorder. *Psychoradiology* **3**, kkad027, doi:10.1093/psyrad/kkad027 (2023).
26 Rohr, C. S., Kamal, S. & Bray, S. Building functional connectivity neuromarkers of behavioral self-regulation across children with and without Autism Spectrum Disorder. *Developmental Cognitive Neuroscience* **41**, doi:ARTN 100747 10.1016/j.dcn.2019.100747 (2020).
27 Dufford, A., Kimble, V., Tejavibulya, L., Dadashkarimi, J. & Scheinost, D. Predicting Transdiagnostic Social Impairments in Childhood Using Connectome-Based Predictive Modeling. *Biol Psychiat* **91**, S87, doi:10.1016/j.biopsych.2022.02.234 (2022).
28 Horien, C. *et al.* A generalizable connectome-based marker of in-scan sustained attention in neurodiverse youth. *Cereb Cortex* **33**, 6320-6334, doi:10.1093/cercor/bhac506 (2023).
29 Finn, E. S. Is it time to put rest to rest? *Trends Cogn Sci* **25**, 1021-1032, doi:10.1016/j.tics.2021.09.005 (2021).
30 O'Connor, D., Horien, C, Mandino, F, Constable, RT. Identifying dynamic reproducible brain states using a predictive modelling approach. *bioRxiv*, doi:https://doi.org/10.1101/2022.10.14.512147 (2022).
31 Zhang, X., Hulvershorn, LA, Constable, RT, Zhao, Y, Wang, S. Cost efficiency of fMRI studies using resting-state vs task-based functional connectivity. *arXiv*, doi: https://doi.org/10.48550/arXiv.2411.01092 (2024).
32 Ramduny, J. & Kelly, C. Connectome-based fingerprinting: reproducibility, precision, and behavioral prediction. *Neuropsychopharmacology* **50**, 114-123, doi:10.1038/s41386-024-01962-8 (2024).
33 Greene, A. S., Gao, S. Y., Scheinost, D. & Constable, R. T. Task-induced brain state manipulation improves prediction of individual traits. *Nat Commun* **9**, doi:ARTN 2807 10.1038/s41467-018-04920-3 (2018).
34 Jiang, R. T. *et al.* Task-induced brain connectivity promotes the detection of individual differences in brain-behavior relationships. *Neuroimage* **207**, doi:ARTN 116370 10.1016/j.neuroimage.2019.116370 (2020).
35 Greene, A. S., Gao, S., Noble, S., Scheinost, D. & Constable, R. T. How Tasks Change Whole-Brain Functional Organization to Reveal Brain-Phenotype Relationships. *Cell Rep* **32**, 108066, doi:10.1016/j.celrep.2020.108066 (2020).
36 Rosenberg, M. D. *et al.* A neuromarker of sustained attention from whole-brain functional connectivity. *Nat Neurosci* **19**, 165-+, doi:10.1038/nn.4179 (2016).

medRxiv preprint doi: https://doi.org/10.1101/2025.01.14.24319457; this version posted January 17, 2025. The copyright holder for this preprint (which was not certified by peer review) is the author/funder, who has granted medRxiv a license to display the preprint in perpetuity.
It is made available under a CC-BY-NC-ND 4.0 International license .

37 Yoo, K. *et al.* A brain-based general measure of attention. *Nat Hum Behav* **6**, 782-795, doi:10.1038/s41562-022-01301-1 (2022).
38 Ju, S. *et al.* Connectome-based predictive modeling shows sex differences in brain-based predictors of memory performance. *Front Dement* **2**, 1126016, doi:10.3389/frdem.2023.1126016 (2023).
39 Avery, E. W. *et al.* Distributed Patterns of Functional Connectivity Predict Working Memory Performance in Novel Healthy and Memory-impaired Individuals. *J Cognitive Neurosci* **32**, 241-255, doi:10.1162/jocn_a_01487 (2020).
40 Hardikar, S. *et al.* Personality traits vary in their association with brain activity across situations. *Commun Biol* **7**, 1498, doi:10.1038/s42003-024-07061-0 (2024).
41 Finn, E. S. & Bandettini, P. A. Movie-watching outperforms rest for functional connectivity-based prediction of behavior. *Neuroimage* **235**, 117963, doi:10.1016/j.neuroimage.2021.117963 (2021).
42 Finn, E. S. *et al.* Can brain state be manipulated to emphasize individual differences in functional connectivity? *Neuroimage* **160**, 140-151, doi:10.1016/j.neuroimage.2017.03.064 (2017).
43 Keehn, B., Nair, A., Lincoln, A. J., Townsend, J. & Muller, R. A. Under-reactive but easily distracted: An fMRI investigation of attentional capture in autism spectrum disorder. *Dev Cogn Neurosci* **17**, 46-56, doi:10.1016/j.dcn.2015.12.002 (2016).
44 Keehn, B., Shih, P., Brenner, L. A., Townsend, J. & Muller, R. A. Functional connectivity for an "Island of sparing" in autism spectrum disorder: An fMRI study of visual search. *Hum Brain Mapp* **34**, 2524-2537, doi:10.1002/hbm.22084 (2013).
45 Vaidya, C. J. *et al.* Controlling attention to gaze and arrows in childhood: an fMRI study of typical development and Autism Spectrum Disorders. *Dev Sci* **14**, 911-924, doi:10.1111/j.1467-7687.2011.01041.x (2011).
46 Rahko, J. S. *et al.* Attention and Working Memory in Adolescents with Autism Spectrum Disorder: A Functional MRI Study. *Child Psychiatry Hum Dev* **47**, 503-517, doi:10.1007/s10578-015-0583-6 (2016).
47 Fitzgerald, J. *et al.* Disrupted functional connectivity in dorsal and ventral attention networks during attention orienting in autism spectrum disorders. *Autism Res* **8**, 136-152, doi:10.1002/aur.1430 (2015).
48 Kernbach, J. M. *et al.* Shared endo-phenotypes of default mode dsfunction in attention deficit/hyperactivity disorder and autism spectrum disorder. *Transl Psychiatry* **8**, 133, doi:10.1038/s41398-018-0179-6 (2018).
49 Stevens T, P. L., Barnard-Brak L. The comorbidity of ADHD in children diagnosed with autism spectrum disorder. *Research in Autism Spectrum Disorders* **31**, 11-18 (2016).
50 Reiersen, A. M. & Todd, R. D. Co-occurrence of ADHD and autism spectrum disorders: phenomenology and treatment. *Expert Rev Neurother* **8**, 657-669, doi:10.1586/14737175.8.4.657 (2008).
51 Antshel, K. M. & Russo, N. Autism Spectrum Disorders and ADHD: Overlapping Phenomenology, Diagnostic Issues, and Treatment Considerations. *Curr Psychiatry Rep* **21**, 34, doi:10.1007/s11920-019-1020-5 (2019).
52 Alvarez-Fernandez, S. *et al.* Perceived social support in adults with autism spectrum disorder and attention-deficit/hyperactivity disorder. *Autism Res* **10**, 866-877, doi:10.1002/aur.1735 (2017).

medRxiv preprint doi: https://doi.org/10.1101/2025.01.14.24319457; this version posted January 17, 2025. The copyright holder for this preprint (which was not certified by peer review) is the author/funder, who has granted medRxiv a license to display the preprint in perpetuity.
It is made available under a CC-BY-NC-ND 4.0 International license .

53 Esterman, M., Noonan, S. K., Rosenberg, M. & DeGutis, J. In the Zone or Zoning Out? Tracking Behavioral and Neural Fluctuations During Sustained Attention. *Cereb Cortex* **23**, 2712-2723, doi:10.1093/cercor/bhs261 (2013).

54 Rosenberg, M., Noonan, S., DeGutis, J. & Esterman, M. Sustaining visual attention in the face of distraction: a novel gradual-onset continuous performance task. *Atten Percept Psycho* **75**, 426-439, doi:10.3758/s13414-012-0413-x (2013).

55 Chawarska, K., Macari, S. & Shic, F. Context modulates attention to social scenes in toddlers with autism. *J Child Psychol Psychiatry* **53**, 903-913, doi:10.1111/j.1469-7610.2012.02538.x (2012).

56 Chawarska, K., Macari, S. & Shic, F. Decreased spontaneous attention to social scenes in 6-month-old infants later diagnosed with autism spectrum disorders. *Biol Psychiatry* **74**, 195-203, doi:10.1016/j.biopsych.2012.11.022 (2013).

57 Shic, F., Macari, S. & Chawarska, K. Speech disturbs face scanning in 6-month-old infants who develop autism spectrum disorder. *Biol Psychiatry* **75**, 231-237, doi:10.1016/j.biopsych.2013.07.009 (2014).

58 Shic, F., Wang, Q., Macari, S. L. & Chawarska, K. The role of limited salience of speech in selective attention to faces in toddlers with autism spectrum disorders. *J Child Psychol Psychiatry* **61**, 459-469, doi:10.1111/jcpp.13118 (2020).

59 Campbell, D. J., Shic, F., Macari, S. & Chawarska, K. Gaze response to dyadic bids at 2 years related to outcomes at 3 years in autism spectrum disorders: a subtyping analysis. *J Autism Dev Disord* **44**, 431-442, doi:10.1007/s10803-013-1885-9 (2014).

60 Horien, C. *et al.* Low-motion fMRI data can be obtained in pediatric participants undergoing a 60-minute scan protocol. *Sci Rep-Uk* **10**, doi:ARTN 21855 10.1038/s41598-020-78885-z (2020).

61 Ingersoll, B. Broader autism phenotype and nonverbal sensitivity: evidence for an association in the general population. *J Autism Dev Disord* **40**, 590-598, doi:10.1007/s10803-009-0907-0 (2010).

62 Lord C, R. M., DiLavore PC, Risi S, Gotham K, Bishop S. *Autism Diagnostic Observation Schedule, Second Edition.*, (Western Psychological Services, 2012).

63 Greene, A. S. *et al.* Brain-phenotype models fail for individuals who defy sample stereotypes. *Nature* **609**, 109-118, doi:10.1038/s41586-022-05118-w (2022).

64 Horien, C. *et al.* Considering factors affecting the connectome-based identification process: Comment on Waller et al. *Neuroimage* **169**, 172-175, doi:10.1016/j.neuroimage.2017.12.045 (2018).

65 Rapuano, K. M. *et al.* Behavioral and brain signatures of substance use vulnerability in childhood. *Dev Cogn Neurosci* **46**, 100878, doi:10.1016/j.dcn.2020.100878 (2020).

66 Dufford, A. J. *et al.* Predicting Transdiagnostic Social Impairments in Childhood using Connectome-based Predictive Modeling. *medRxiv*, 2022.2004.2007.22273518, doi:10.1101/2022.04.07.22273518 (2022).

67 Scheinost, D. *et al.* Functional connectivity during frustration: a preliminary study of predictive modeling of irritability in youth. *Neuropsychopharmacology* **46**, 1300-1306, doi:10.1038/s41386-020-00954-8 (2021).

68 Taxali, A., Angstadt, M., Rutherford, S. & Sripada, C. Boost in Test-Retest Reliability in Resting State fMRI with Predictive Modeling. *Cereb Cortex* **31**, 2822-2833, doi:10.1093/cercor/bhaa390 (2021).

medRxiv preprint doi: https://doi.org/10.1101/2025.01.14.24319457; this version posted January 17, 2025. The copyright holder for this preprint (which was not certified by peer review) is the author/funder, who has granted medRxiv a license to display the preprint in perpetuity.
It is made available under a CC-BY-NC-ND 4.0 International license .

69 Birn, R. M. *et al.* The effect of scan length on the reliability of resting-state fMRI connectivity estimates. *Neuroimage* **83**, 550-558, doi:10.1016/j.neuroimage.2013.05.099 (2013).
70 Laumann, T. O. *et al.* Functional System and Areal Organization of a Highly Sampled Individual Human Brain. *Neuron* **87**, 657-670, doi:10.1016/j.neuron.2015.06.037 (2015).
71 Noble, S. *et al.* Influences on the Test-Retest Reliability of Functional Connectivity MRI and its Relationship with Behavioral Utility. *Cereb Cortex* **27**, 5415-5429, doi:10.1093/cercor/bhx230 (2017).
72 Steegen, S., Tuerlinckx, F., Gelman, A. & Vanpaemel, W. Increasing Transparency Through a Multiverse Analysis. *Perspect Psychol Sci* **11**, 702-712, doi:10.1177/1745691616658637 (2016).
73 Di Martino, A. *et al.* Data Descriptor: Enhancing studies of the connectome in autism using the autism brain imaging data exchange II. *Scientific Data* **4**, doi:ARTN 170010 10.1038/sdata.2017.10 (2017).
74 Di Martino, A. *et al.* The autism brain imaging data exchange: towards a large-scale evaluation of the intrinsic brain architecture in autism. *Molecular Psychiatry* **19**, 659-667, doi:10.1038/mp.2013.78 (2014).
75 Constantino, J. N. *et al.* Validation of a brief quantitative measure of autistic traits: comparison of the social responsiveness scale with the autism diagnostic interview-revised. *J Autism Dev Disord* **33**, 427-433, doi:10.1023/a:1025014929212 (2003).
76 Koshino, H. *et al.* Functional connectivity in an fMRI working memory task in high-functioning autism. *Neuroimage* **24**, 810-821, doi:10.1016/j.neuroimage.2004.09.028 (2005).
77 Keehn, B., Shih, P., Brenner, L. A., Townsend, J. & Muller, R. A. Functional connectivity for an "island of sparing" in autism spectrum disorder: an fMRI study of visual search. *Hum Brain Mapp* **34**, 2524-2537, doi:10.1002/hbm.22084 (2013).
78 McGrath, J. *et al.* Atypical visuospatial processing in autism: insights from functional connectivity analysis. *Autism Res* **5**, 314-330, doi:10.1002/aur.1245 (2012).
79 Gilbert, S. J., Bird, G., Brindley, R., Frith, C. D. & Burgess, P. W. Atypical recruitment of medial prefrontal cortex in autism spectrum disorders: an fMRI study of two executive function tasks. *Neuropsychologia* **46**, 2281-2291, doi:10.1016/j.neuropsychologia.2008.03.025 (2008).
80 Just, M. A., Cherkassky, V. L., Keller, T. A., Kana, R. K. & Minshew, N. J. Functional and anatomical cortical underconnectivity in autism: evidence from an FMRI study of an executive function task and corpus callosum morphometry. *Cereb Cortex* **17**, 951-961, doi:10.1093/cercor/bhl006 (2007).
81 Knaus, T. A., Silver, A. M., Lindgren, K. A., Hadjikhani, N. & Tager-Flusberg, H. fMRI activation during a language task in adolescents with ASD. *J Int Neuropsychol Soc* **14**, 967-979, doi:10.1017/S1355617708081216 (2008).
82 Greene, A. S., Horien, C., Barson, D., Scheinost, D. & Constable, R. T. Why is everyone talking about brain state? *Trends Neurosci* **46**, 508-524, doi:10.1016/j.tins.2023.04.001 (2023).
83 Finn, E. S. & Rosenberg, M. D. Beyond fingerprinting: Choosing predictive connectomes over reliable connectomes. *Neuroimage* **239**, 118254, doi:10.1016/j.neuroimage.2021.118254 (2021).

medRxiv preprint doi: https://doi.org/10.1101/2025.01.14.24319457; this version posted January 17, 2025. The copyright holder for this preprint (which was not certified by peer review) is the author/funder, who has granted medRxiv a license to display the preprint in perpetuity.
It is made available under a CC-BY-NC-ND 4.0 International license .

84 Rai, S., Graff, K., Tansey, R. & Bray, S. How do tasks impact the reliability of fMRI functional connectivity? *Hum Brain Mapp* **45**, e26535, doi:10.1002/hbm.26535 (2024).

85 Greene, A. S., Gao, S. Y., Noble, S., Scheinost, D. & Constable, R. T. How Tasks Change Whole-Brain Functional Organization to Reveal Brain-Phenotype Relationships. *Cell Rep* **32**, doi:ARTN 108066
10.1016/j.celrep.2020.108066 (2020).

86 Sripada, C., Angstadt, M., Rutherford, S., Taxali, A. & Shedden, K. Toward a "treadmill test" for cognition: Improved prediction of general cognitive ability from the task activated brain. *Hum Brain Mapp* **41**, 3186-3197, doi:10.1002/hbm.25007 (2020).

87 Di Martino, A. *et al.* Shared and distinct intrinsic functional network centrality in autism and attention-deficit/hyperactivity disorder. *Biol Psychiatry* **74**, 623-632, doi:10.1016/j.biopsych.2013.02.011 (2013).

88 Itahashi, T. *et al.* Neural correlates of shared sensory symptoms in autism and attention-deficit/hyperactivity disorder. *Brain Commun* **2**, fcaa186, doi:10.1093/braincomms/fcaa186 (2020).

89 Harikumar, A., Evans, D. W., Dougherty, C. C., Carpenter, K. L. H. & Michael, A. M. A Review of the Default Mode Network in Autism Spectrum Disorders and Attention Deficit Hyperactivity Disorder. *Brain Connect* **11**, 253-263, doi:10.1089/brain.2020.0865 (2021).

90 Ames C, F.-W. S. A review of methods in the study of attention in autism. *Developmental Review* **30**, 52-73 (2010).

91 Segura, P. *et al.* Connectome-based symptom mapping and in silico related gene expression in children with autism and/or attention-deficit/hyperactivity disorder. *medRxiv*, 2024.2012.2009.24318621, doi:10.1101/2024.12.09.24318621 (2024).

92 Chou, Y. H. *et al.* Maintenance and Representation of Mind Wandering during Resting-State fMRI. *Sci Rep* **7**, 40722, doi:10.1038/srep40722 (2017).

93 Bettoni, R. *et al.* Learning and generalization of repetition-based rules in autism. *Psychol Res* **87**, 1429-1438, doi:10.1007/s00426-022-01761-0 (2023).

94 Yerys, B. E. *et al.* The fMRI Success Rate of Children and Adolescents: Typical Development, Epilepsy, Attention Deficit/Hyperactivity Disorder, and Autism Spectrum Disorders. *Human Brain Mapping* **30**, 3426-3435, doi:10.1002/hbm.20767 (2009).

95 Pardoe, H. R., Kucharsky Hiess, R. & Kuzniecky, R. Motion and morphometry in clinical and nonclinical populations. *Neuroimage* **135**, 177-185, doi:10.1016/j.neuroimage.2016.05.005 (2016).

96 Yao, N. *et al.* Inferring pathobiology from structural MRI in schizophrenia and bipolar disorder: Modeling head motion and neuroanatomical specificity. *Hum Brain Mapp* **38**, 3757-3770, doi:10.1002/hbm.23612 (2017).

97 Tansey, R. *et al.* Functional MRI responses to naturalistic stimuli are increasingly typical across early childhood. *Dev Cogn Neurosci* **62**, 101268, doi:10.1016/j.dcn.2023.101268 (2023).

98 Tansey, R. *et al.* Inattentive and hyperactive traits differentially associate with interindividual functional synchrony during video viewing in young children without ADHD. *Cereb Cortex Commun* **3**, tgac011, doi:10.1093/texcom/tgac011 (2022).

99 Bagheri, S. *et al.* Transdiagnostic Neurobiology of Social Cognition and Individual Variability as Measured by Fractional Amplitude of Low-Frequency Fluctuation in

medRxiv preprint doi: https://doi.org/10.1101/2025.01.14.24319457; this version posted January 17, 2025. The copyright holder for this preprint (which was not certified by peer review) is the author/funder, who has granted medRxiv a license to display the preprint in perpetuity.
It is made available under a CC-BY-NC-ND 4.0 International license .

Schizophrenia and Autism Spectrum Disorders. *bioRxiv*, 2024.2007.2002.601737, doi:10.1101/2024.07.02.601737 (2024).
100 Itahashi, T. *et al.* Generalizable and transportable resting-state neural signatures characterized by functional networks, neurotransmitters, and clinical symptoms in autism. *Mol Psychiatry*, doi:10.1038/s41380-024-02759-3 (2024).
101 Gordon, E. M. *et al.* Precision Functional Mapping of Individual Human Brains. *Neuron* **95**, 791-807 e797, doi:10.1016/j.neuron.2017.07.011 (2017).
102 Lombardo, M. V., Lai, M. C. & Baron-Cohen, S. Big data approaches to decomposing heterogeneity across the autism spectrum. *Molecular Psychiatry* **24**, 1435-1450, doi:10.1038/s41380-018-0321-0 (2019).
103 Marek, S. *et al.* Reproducible brain-wide association studies require thousands of individuals. *Nature* **603**, 654-660, doi:10.1038/s41586-022-04492-9 (2022).
104 Pua, E. P. K., Barton, S., Williams, K., Craig, J. M. & Seal, M. L. Individualised MRI training for paediatric neuroimaging: A child-focused approach. *Dev Cogn Neurosci* **41**, 100750, doi:10.1016/j.dcn.2019.100750 (2020).
105 de Bie, H. M. *et al.* Preparing children with a mock scanner training protocol results in high quality structural and functional MRI scans. *Eur J Pediatr* **169**, 1079-1085, doi:10.1007/s00431-010-1181-z (2010).
106 Rosenberg, M. D. & Finn, E. S. How to establish robust brain-behavior relationships without thousands of individuals. *Nat Neurosci* **25**, 835-837, doi:10.1038/s41593-022-01110-9 (2022).
107 Spisak, T., Bingel, U. & Wager, T. D. Multivariate BWAS can be replicable with moderate sample sizes. *Nature* **615**, E4-E7, doi:10.1038/s41586-023-05745-x (2023).
108 Kang, K. *et al.* Study design features increase replicability in brain-wide association studies. *Nature*, doi:10.1038/s41586-024-08260-9 (2024).
109 Kiar, G. *et al.* Why experimental variation in neuroimaging should be embraced. *Nat Commun* **15**, 9411, doi:10.1038/s41467-024-53743-y (2024).
110 Bedford, S. A. *et al.* Large-scale analyses of the relationship between sex, age and intelligence quotient heterogeneity and cortical morphometry in autism spectrum disorder. *Mol Psychiatry* **25**, 614-628, doi:10.1038/s41380-019-0420-6 (2020).
111 Lai, M. C. *et al.* Imaging sex/gender and autism in the brain: Etiological implications. *J Neurosci Res* **95**, 380-397, doi:10.1002/jnr.23948 (2017).
112 Floris, D. L. *et al.* Towards robust and replicable sex differences in the intrinsic brain function of autism. *Mol Autism* **12**, 19, doi:10.1186/s13229-021-00415-z (2021).
113 Chouinard, B., Gallagher, L. & Kelly, C. He said, she said: Autism spectrum diagnosis and gender differentially affect relationships between executive functions and social communication. *Autism* **23**, 1793-1804, doi:10.1177/1362361318815639 (2019).
114 Joshi, A. *et al.* Unified framework for development, deployment and robust testing of neuroimaging algorithms. *Neuroinformatics* **9**, 69-84, doi:10.1007/s12021-010-9092-8 (2011).
115 Lutkenhoff, E. S. *et al.* Optimized brain extraction for pathological brains (optiBET). *Plos One* **9**, e115551, doi:10.1371/journal.pone.0115551 (2014).
116 Finn, E. S. *et al.* Functional connectome fingerprinting: identifying individuals using patterns of brain connectivity. *Nat Neurosci* **18**, 1664-1671, doi:10.1038/nn.4135 (2015).

medRxiv preprint doi: https://doi.org/10.1101/2025.01.14.24319457; this version posted January 17, 2025. The copyright holder for this preprint (which was not certified by peer review) is the author/funder, who has granted medRxiv a license to display the preprint in perpetuity.
It is made available under a CC-BY-NC-ND 4.0 International license .

117 Satterthwaite, T. D. *et al.* An improved framework for confound regression and filtering for control of motion artifact in the preprocessing of resting-state functional connectivity data. *Neuroimage* **64**, 240-256, doi:10.1016/j.neuroimage.2012.08.052 (2013).
118 Scheinost, D. *et al.* Ten simple rules for predictive modeling of individual differences in neuroimaging. *Neuroimage* **193**, 35-45, doi:10.1016/j.neuroimage.2019.02.057 (2019).
119 Benjamini, Y., Hochberg, Y. Controlling the false discovery rate: a practical and powerful approach to multiple testing. *Journal of the Royal Statistical Society*, *Series B* **57**, 289-300 (1995).
120 Yip, S. W., Scheinost, D., Potenza, M. N. & Carroll, K. M. Connectome-Based Prediction of Cocaine Abstinence. *Am J Psychiatry* **176**, 156-164, doi:10.1176/appi.ajp.2018.17101147 (2019).
121 Rosenberg, M. D. *et al.* Methylphenidate Modulates Functional Network Connectivity to Enhance Attention. *J Neurosci* **36**, 9547-9557, doi:10.1523/Jneurosci.1746-16.2016 (2016).
122 Ju, Y. *et al.* Connectome-based models can predict early symptom improvement in major depressive disorder. *J Affect Disord* **273**, 442-452, doi:10.1016/j.jad.2020.04.028 (2020).